



Laboratory and Numerical Studies of Water Flow Through Selected Fittings Installed at Copper Pipelines

Oktawia Pliżga, Beata Kowalska, Anna Musz-Pomorska
Lublin University of Technology

1. Introduction

Minor losses in domestic installations, water supply or heating, directly connected to the pipelines materials and applied fittings, may cause significant pressure losses. The proper and exact determination of minor losses may become a serious engineering task. Numerous scientific reports (Cisowska et al. 2004, Chern et al. 2007, Strzelecka & Jeżowiecka-Kabsch 2008, 2010, Shirazi et al. 2012, Widomski et al. 2012) showed that traditional methodology, based on former PN-M-34034:1976 standard, repeated also e.g. in the actual PE-EN 1267:2012, applied to installations consisting of pipelines and fittings of various materials (metals and polymers/plastics) often gave results far from the actual, measured values. Nowadays, determination of minor losses during designing of modern domestic installations based on plastic pipelines is generally performed on the basis of values of coefficients supported by the producers of pipelines and fittings (Piechurski et al. 2009, Widomski et al. 2012, Janowska et al. 2013).

There are still unanswered questions concerning how the supported values meet the complicated and multivariate cases of various fittings at flow of different Reynolds numbers.

Table 1 presents standards values of minor loss coefficients for 90° long elbow and full crossover reported in literature or suggested in technical guidelines.

Table 1. Literature values of minor loss coefficients for long elbow and full crossover

Tabela 1. Wartości literaturowe oporów miejscowych dla łuku i odsadzki

Source	Górecki et al. 2009	Strzeszewski 2010	COBRTI Instal 2004	DIN 1988	PCPM 2013
Long elbow	1.0	1.0	0.7	0.7	1.0
Full crossover	0.5	0.5	0.5	0.5	0.5

As it can be seen in Tab. 1, known technical guidelines, standards and literature reports suggest constant value of minor loss coefficient, despite the fact that variable flow conditions may occur inside water supply or heating domestic installation.

Numerical modeling based on Computational Fluid Dynamics (CFD) seems to be a useful tool in the assessment of phenomena occurring during water flow through various piping and fittings and determination of minor loss coefficients for variable Re number. CFD was successfully applied in many benches of science and technology, including numerical modeling of hydraulic parameters for water flow inside water supply installations and networks (Musz et al. 2009, Widomski et al. 2012, Janowska et al. 2013, Musz et al. 2015). The commercial Fluent, Ansys Inc. is a worldwide known CFD computing software popularly used in various studies concerning water flow (Ahmad et al. 2005, Liu & Peng 2005, Norton & Sun 2006).

This paper presents results of laboratory and numerical studies concerning pressure losses at variable Reynolds number for the selected fittings installed at copper installation pipes. Our studies were conducted for 90° long elbow and full crossover 15 x 1 mm installed at pipeline by soft soldering. Numerical calculations performed in Fluent, Ansys Inc., were used to analyze the distribution of flow velocity magnitude and turbulence intensity during water flow through the studied fittings, as well as to calculate the minor loss coefficient for a given volumetric flow rate and Reynolds number.

2. Materials and methods

Studies concerning values of minor pressure loss related to water flow rate were performed for copper 90 degree long elbow DN 15x1 and

copper full crossover DN 15x1. Both tested fittings were installed at the pipeline by soft soldering.

Laboratory measurements of water flow through the tested fittings were performed at the laboratory setup specially constructed for this purpose, presented in Fig. 1. The spatial arrangement of pressure measurements points and length of the used straight segments of pipelines before and after the tested fittings were based on the literature reports (Siwiec et al. 2002, Cisowska & Kotowski 2004, 2006, Grajper & Smółka 2010, Strzelecka & Jeżowiecka-Kabsch 2010, Wienerowska-Bords 2014, Dul et al. 2015) and met the requirements of PN-EN 1267:2012; they are longer than the required $\geq 2D$ before and $\geq 10D$ after the location of minor pressure loss. The applied measurement installation was consisting of set of rotameters, copper pipelines DN 15x1, tested fittings, air removal valve and pressure measurement unit, i.e. differential manometer of accuracy 0.01 m H₂O. Measurements were performed for increasing and decreasing volumetric flow rate within the range of 100 to 1400 dm³·h⁻¹, with the step of 50 dm³·h⁻¹.

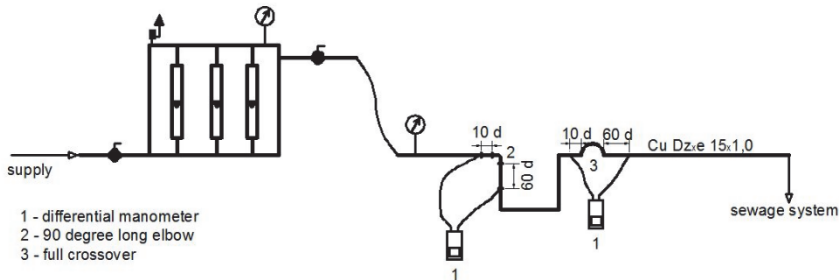


Fig. 1. Scheme of laboratory setup

Rys. 1. Schemat stanowiska pomiarowego

Numerical calculations of water flow through the tested fittings were performed in CFD computing software FLUENT 6, ANSYS 12.0.16 Inc., USA, on the basis of the finite volume method. The developed geometrical models, reflected water body filling the tested installation, taking into consideration the precise mapping of tested fittings and applied joints in the scale of similarity 1:1.

In both cases, the 3D discretization based on pyramidal finite elements/volumes shape was applied to evolve the finite elements mesh.

The number of developed elements and nodes reached the level of approx. 160 000 and 34 500 for long elbow and 1 200 000 and 240 000 for full crossover, respectively.

The applied numerical calculations of water flow through the tested fittings were based on the standard two-equation k-epsilon turbulence model (Launder & Spalding 1974). The described numerical calculations of water flow through the long elbow and full crossover were performed for variable Reynolds number, greater than 20 000, i.e. for volumetric flow rate within the range 1000-1400 dm³·h⁻¹. The applied input data for numerical modeling covered density of water in range 998.3-998.9 kg·m⁻³ and viscosity 0.001 do 0.0011 kg·m⁻¹·s⁻¹, both in relation to observed water temperature during measurements. The assumed boundary conditions at the inflow to the developed model covered variable mass flow rate, static gage pressure equal to 1.2 bar and variable initial turbulence intensity. Wall boundary condition was determined as pipe wall material roughness equal to 1.5·10⁻³ mm. The outflow boundary condition required the value of atmospheric pressure to be assigned; hence, the standard atmospheric pressure equal to 101325 Pa was set.

The assumed as inflow boundary condition turbulence intensity was determined according to the equation below (Wesseling 2000):

$$I = 0.16 \cdot \text{Re}^{\frac{1}{8}} \quad (1)$$

where: I – turbulence intensity [%].

Determination of coefficient of minor loss for tested fittings, obtained by both applied methods, laboratory measurements and numerical modeling, was based on a transformed Bernoulli's equation for straight, horizontal pipeline of constant diameter. Value of friction factor for Darcy-Weisbach equation was determined separately for each case by iteration method according to Colebrook-White equation.

3. Results and discussion

Results of laboratory measurements of pressure loss, in relation to Reynolds number, during water flow through the tested fittings were presented in Fig. 2. A clear relation between value of Reynolds number, resulting from increasing flow rate, and the measured value of pressure

loss for each of the studied fitting is visible in Fig. 2. The greater increase of pressure loss was observed for the studied 90° long elbow. The maximum observed pressure loss was equal 13.7 kPa for Reynolds number $Re = 30794$ ($v = 3.1 \text{ m}\cdot\text{s}^{-1}$).

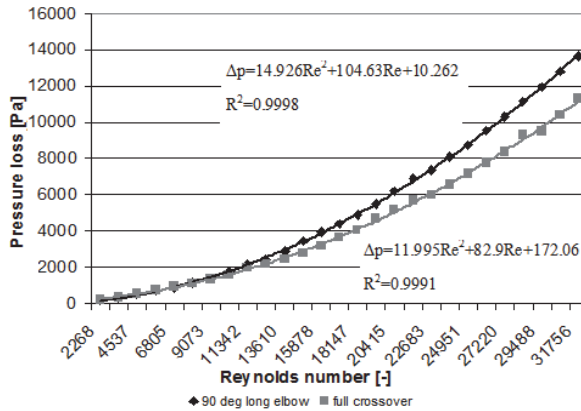


Fig. 2. Measured pressure drop for the tested long elbow and full crossover as function of Reynolds number

Rys. 2. Pomierzone wartości straty ciśnienia w funkcji liczby Reynoldsa

Fig. 3 and Fig. 4 present measured values of minor loss coefficient for 90° long elbow and full crossover as a function of Reynolds number.

Results of the performed laboratory measurements showed a clear relation between Reynolds number ($Re < 10\,000$, mean inflow velocity value equal $2.09 \text{ m}\cdot\text{s}^{-1}$) and the observed pressure loss, as well as the coefficients of minor losses. The type of flow reflected by the value of the Reynolds number as well as value of the resultant friction pressure losses may affect the minor pressure loss at low values of Re number. In our case, for $Re < 10\,000$, taking into account that k/D ratio for the applied pipes was approx. equal to $1 \cdot 10^{-4}$, the studied pipeline may be treated as nearly hydraulically smooth (as it is presented in the Nikuradse's graph) for which the constant reduction in the value of friction factor for the increasing Re number may be observed. Thus, decreasing value of the measured coefficient of minor pressure loss for $Re < 10\,000$ is comprehensible.

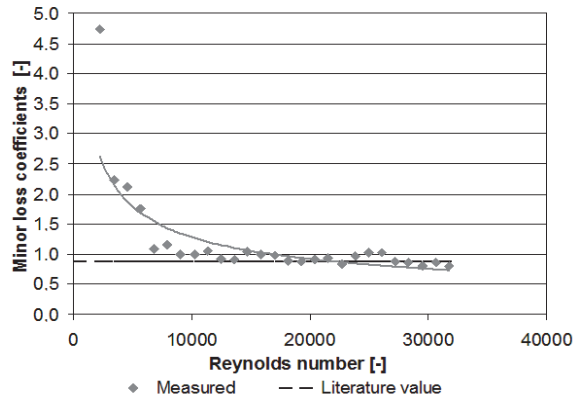


Fig. 3. Results of modeled and measured minor loss coefficients for 90° long elbow; where solid line – is an approximated function

Rys. 3. Pomierzone i obliczone wartości współczynników strat miejscowych dla łuku 90°; linia ciągła – funkcja aproksymacyjna

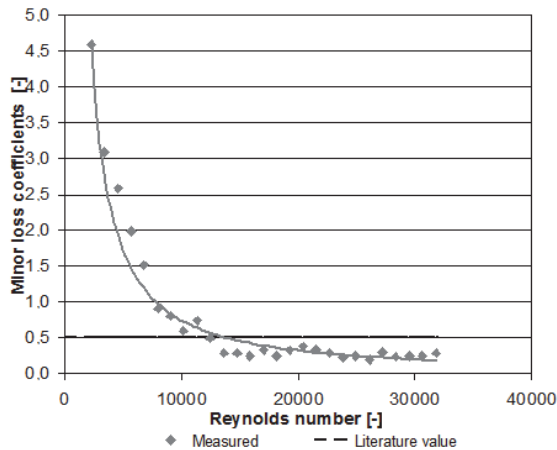


Fig. 4. Results of modeled and measured minor loss coefficients for full crossover; where solid line – is an approximated function

Rys. 4. Pomierzone i obliczone wartości współczynników strat miejscowych dla odsadzki; linia ciągła – funkcja aproksymacyjna

For the water flow characterized by approx. $Re > 10\,000$, the measured coefficients of minor loss for both tested fittings showed a nearly constant value (0.92 for long elbow and 0.31 for full crossover).

Thus, in case of 90° long elbow, the presented value of minor loss for $Re > 10\,000$ is greater by 0.02, i.e. 2.2%, than the average literature value, while for full crossover it was lower by 0.2, i.e. 38% of difference.

The results of the performed numerical modeling for high Reynolds number, i.e. $Re > 20\,000$ fully confirmed the presented observations. The exemplary visualizations of numerical modeling results of velocity of flow magnitude and turbulence intensity for long elbow were presented in Fig. 5.

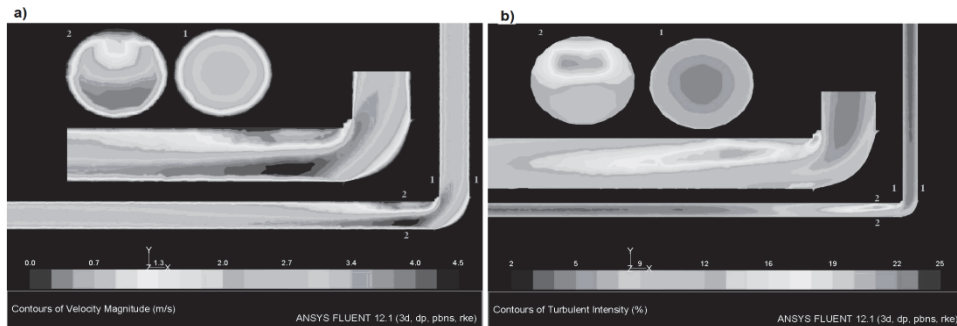


Fig. 5. Contours of velocity magnitude [$\text{m}\cdot\text{s}^{-1}$] for two longitudinal cross sections (a) and spatial distribution of turbulent intensity (b) of the tested long elbow for flow rate equal to $1400\text{ dm}^3\cdot\text{h}^{-1}$

Rys. 5. Układ przestrzenny wypadkowej prędkości [$\text{m}\cdot\text{s}^{-1}$] w dwóch przekrojach podłużnych (a) oraz rozkład intensywności turbulencji (b) dla łuku, dla natężenia przepływu $1400\text{ dm}^3\cdot\text{h}^{-1}$

The spatial distributions of velocity magnitude and turbulent intensity for exemplary volumetric flow rate equal to $1400\text{ m}^3/\text{h}$ presented in Fig. 5 explain the reasons of minor loss generation for tested fittings and joints. The maximum values of velocity magnitude and turbulence intensity observed reached the values of 4.5 m/s and 22% for the 90° long elbow and 4.7 m/s and 21% for the full crossover, respectively. The value of turbulence intensity equal to 5% is a typical value assumed for undisturbed water flow (Wesseling 2000, Minkowycz et al. 2009). Thus, momentum changes and additional turbulences caused by changes of flow stream shape, stream contraction and boundary layer separation, visible in Fig 5, result in a local pressure drop.

The full range of variability of maximum modeled local velocity magnitude, turbulence intensity and obtained values of minor loss coeffi-

icients for all modeled values of volumetric flow rate characterized by $Re > 20\,000$.

Table 2. Results of numerical modeling covering maximum velocity magnitude, turbulence intensity and minor pressure loss coefficient for the tested volumetric flow rates

Tabela 2. Wyniki obliczeń modelowych obejmujące maksymalną prędkość, intensywność turbulencji i współczynnik strat ciśnienia dla badanych natężeń przepływu

Flow		Long elbow			Full crossover		
Q [m ³ ·h ⁻¹]	Re [-]	v _{max} [m·s ⁻¹]	I _{max} [%]	ζ [-]	v _{max} [m·s ⁻¹]	I _{max} [%]	ζ [-]
1000	21996	3.2	16	0.92	3.3	16	0.23
1050	23096	3.3	16	0.92	3.5	16	0.22
1100	24195	3.5	17	0.94	3.6	17	0.20
1150	25295	3.7	18	0.93	3.8	18	0.27
1200	26395	3.8	19	0.91	4.0	18	0.23
1250	27495	4.0	19	0.92	4.2	20	0.31
1300	28595	4.2	20	0.88	4.4	20	0.16
1350	29694	4.3	21	0.93	4.5	21	0.20
1400	30794	4.5	22	0.91	4.7	21	0.23

Results of numerical studies presented in Tab. 2 confirm the observations from laboratory part of our research that for high values (mean inflow velocity values were in range 2.09 and 2.93 m·s⁻¹) of flow velocity and rate, the observed values of minor loss coefficient were nearly constant, despite the increased turbulence intensity. The mean values of modeled minor loss coefficient were equal to 0.92 and 0.23 for the tested long elbow and full crossover, respectively.

The results of numerical modeling were validated by the comparison of calculated values of minor loss coefficients to values obtained by the performed laboratory measurements. Table 3 presents the results of model validation.

Table 3. Validation results for developed numerical model**Tabela 3.** Wyniki walidacji opracowanego modelu

Selected fittings	RSME	R ²	NSE
90 deg long elbow	0.03	0.97	0.978
Full crossover	0.02	0.79	0.798

The presented results of model validation, based on RSME, R² and NSE calculations, showed a satisfactory and acceptable agreement between the modeled and measured values.

4. Conclusions

The performed laboratory and modeling studies concerning the water flow through DN 15x1 mm Cu 90° long elbow and full crossover showed that values of pressure loss and coefficients of minor pressure losses are in some part related to water flow rate and, as it could be expected, to Reynolds number. A clear decreasing relation between minor loss coefficient and Reynolds number for approx. $Re < 10\,000$ was observed. Measured values of minor pressure loss for Reynolds number within range 2000-10 000 decreased from 4.73 to 1.0 for long elbow and from 4.59 to 0.79 for full crossover, respectively. Then, for $Re > 10\,000$, the values of determined coefficients of minor losses stabilized at the level of approx. 0.92 for long elbow and 0.31 for full crossover and were different than the values available in literature and designing guidelines. The obtained results suggest that assumption of constant values of minor loss coefficients for designing calculations for $Re < 10\,000$ may result in significant differences between the calculated and actual values of pressure loss.

Results of our numerical studies confirmed a nearly constant value of minor pressure loss coefficient for significant values of flow velocity and flow rate, resulting in $Re > 20\,000$. Thus, the increasing value of pressure loss for tested fittings for high Re numbers is a result of an increased turbulence intensity triggered by the increase of velocity of flow.

Validation of numerical modeling, based on the comparison of laboratory measurements and numerical modeling results and RSME, R² and NSE calculations, showed a satisfactory agreement between the modeled and measured values.

References

- Ahmad, A.L., Lau, K.K., Bakar, A., Shukor, A. (2005). Integrated CFD simulation of concentration polarization in narrow membrane channel. *Computers and Chemical Engineering*, 29, 2087-2095.
- Chern, M.J., Wang, C.C., Ma, C.H. (2007). Performance test and flow visualization of ball valve. *Experimental Thermal and Fluid Science*, 31, 505-512.
- Cisowska, I., Kotowski, A. (2004). Straty ciśnienia w układach kształtek z polipropylenu. *Gaz, Woda i Technika Sanitarna*, 10, 340-345.
- Cisowska, I., Kotowski, A. (2006). Studies of hydraulic resistance in polypropylene pipes and pipe fittings. *Foundations of Civil and Environmental Engineering*, 8, 37-57.
- COBRTI Instal, Wytyczne techniczne, zeszyt 10. (2004). *Wytyczne projektowania i stosowania instalacji z rur miedzianych*. Warszawa: Instal (TIB).
- DIN 1988-300:2012-05 Technische Regeln für Trinkwasser-Installationen—Teil 300: Ermittlung der Rohrdurchmesser*. Technische Regel des DVGW.
- Dul, K., Widomski, M.K., Musz, A. (2015). Analiza numeryczna przepływu wody przez zawór kulowy zamontowany na przewodzie PEX-AL.-PEX. *Instal*, 11, 36-39.
- Górecki, A., Fedorczyk, Z., Płachta, J., Płuciennik, M., Rutkiewicz A., Stefański W., Zimmer, J. (2009). *Instalacje wodociągowe, ogrzewcze i gazowe na paliwo gazowe wykonane z rur miedzianych. Wytyczne stosowania i projektowania*. Polskie Centrum Promocji Miedzi.
- Grajper, P., Smółka, J. (2010). Eksperymentalne i numeryczne określenie miejscowych strat ciśnienia w kolanach 90° instalacji wodociągowych. *Gaz, Woda i technika Sanitarna*, 7-8, 13-19.
- Janowska, J., Widomski, M.K., Iwanek, M., Musz, A. (2013). *Numerical modeling of water flow through straight globe valve*. In: Environmental Engineering IV: Conference on Environmental Engineering IV; [Eds:] Pawłowski Artur, Dudzińska Marzenna, Pawłowski Lucjan – Boca Raton: CRC Press-Taylor & Francis Group: 41-49.
- Lauder, B.E., Spalding, D.B. (1974). Application of the Energy Dissipation Model of Turbulence to the Calculation of Flow Near a Spinning Disc. *Letters in Heat and Mass Transfer*, 1(2), 131-138.
- Liu, S.X., Peng, M. (2005). Verification of mass transfer simulation with CFD using highly accurate solutions. *Computers and Electronics in Agriculture*, 49, 309-314.
- Minkowycz, W.J., Abraham, J.P., Sparrow, E.M. (2009). Numerical simulation of laminar breakdown and subsequent intermittent and turbulent flow in parallel-plate channels: Effects of inlet velocity profile and turbulence intensity. *International Journal of Heat and Mass Transfer*, 52, 4040-4046.

- Musz, A., Kowalska, B., Widomski, M.K. (2009). Some issues concerning the problems of water quality modeling in distribution systems. *Ecological Chemistry and Engineering S*, 16 (S2), 175-184.
- Musz, A., Widomski, M.K., Kowalska, B. (2015). Benzene propagation during turbulent flow in PE-HD water supply pipes. *Environment Protection Engineering*, 41(4), 5-16.
- Norton, T., Sun, D.W. (2006). Computational fluid dynamics (CFD) e an effective and efficient design and analysis tool for the food industry: A review. *Trends in Food Science & Technology*, 17, 600-620.
- Piechurski, F.G. (2009). *Badanie wpływu połączeń na wzrost współczynnika strat liniowych λ , oraz współczynnika chropowatości bezwzględnej k dla rur instalacyjnych z polipropylenu*. Instalacje wodociągowe i kanalizacyjne. III Konferencja Naukowo-Techniczna, Warszawa-Dębe.
- PN-76-M-34034 Rurociągi – Zasady obliczeń strat ciśnienia.
- PN-EN 1267:2012 Armatura przemysłowa – Badanie oporu przepływu wodą.
- Polskie Centrum Promocji Miedzi. (2013). Instalacje wodociągowe, ogrzewcze i gazowe na paliwo gazowe, chłodnicze, klimatyzacyjne gazów medycznych oraz próżni wykonane z miedzi i stopów miedzi. Wytyczne stosowania i projektowania. Wrocław.
- Shirazi, N.T., Azizyan, G.R., Akbari, G.H. (2012). CFD analysis of the ball valve performance in presence of cavitation. *Life Science Journal*, 9(4), 1460-1467.
- Siwiec, T., Morawski, D., Karaban, G. (2002). Eksperymentalne badania oporów hydraulicznych w zgrzewanych kształtkach z tworzyw sztucznych. *Gaz, Woda i technika Sanitarna*, 2, 49-50 and 63-68.
- Strzelecka, K., Jeżowiecka-Kabsch, K. (2008). Rzeczywiste wartości współczynnika oporów miejscowych podczas przepływu wody przez skokowe rozszerzenie rury. *Ochrona Środowiska*, 30(2), 29-33.
- Strzelecka, K., Jeżowiecka-Kabsch, K. (2010). Rzeczywiste wartości współczynnika strat miejscowych podczas przepływu wody przez nagłe rozszerzenie rury. *Ochrona Środowiska*, 32(1), 33-37.
- Strzeszewski, M. (2010). *Obliczenia hydrauliczne instalacji centralnego ogrzewania. Materiały do zajęć z ogrzewnictwa*. Warszawa: Politechnika Warszawska.
- Weinerowska-Bords, K. (2014). Eksperymentalna analiza współczynników oporów lokalnych dla wybranych kształtek i złązek w systemach rur wielowarstwowych. *Instal*, 6, 42-49.
- Wesseling, P. (2000). Principles of Computational Fluid Mechanics. *Springer Series in Computational Mathematics*, 29, 167-188.

Widomski, M.K., Kowalska, B., Kowalski, D. (2012). Model Investigations into the Propagation of Butylated Hydroxytoluene (BHT) Migrating from High Density Polyethylene Pipes (HDPE) to Water. *Ochrona Środowiska*, 34(3), 33-37.

Laboratoryjne i modelowe badania przepływu wody przez wybrane opory miejscowe na przewodach miedzianych

Streszczenie

Praca przedstawia badania laboratoryjne oraz analizę numeryczną warunków przepływu wody przez łuk 90° oraz odsadzkę o średnicy 15x1 mm wykonanych z miedzi i połączonych z przewodem miedzianym za pomocą lutu miękkiego. Badania laboratoryjne zrealizowano na specjalnie do tego celu wykonanym stanowisku laboratoryjnym przy natężeniu przepływu wody z zakresu 100-1400 dm³/h. Badania modelowe przeprowadzono z wykorzystaniem komercyjnego pakietu obliczeniowego CFD Ansys Fluent. Wykonane wariantowe badania modelowe obejmowały obserwacje przestrzennego pola prędkości, układu strug, rozkładu intensywności turbulencji oraz określenie straty ciśnienia i współczynnika oporu miejscowego dla zmiennej liczby Reynoldsa. Przeprowadzono obliczenia numeryczne dla przepływów o $Re > 20\ 000$, tj. dla natężeń przepływu z zakresu 1000-1400 dm³/h. Wyniki badań laboratoryjnych wykazały wyraźną zależność pomiędzy liczbą Reynoldsa a zaobserwowanymi stratami ciśnienia oraz współczynnikiem straty miejscowej dla badanych oporów miejscowych. Analiza wyników badań modelowych uwypukliła zależność pomiędzy wielkością straty ciśnienia a układem i osiąganymi wartościami prędkości przepływu oraz intensywności turbulencji dla zmiennej liczby Reynoldsa. Walidacja modelu wykazała zadowalającą zgodność wyników symulacji z wynikami zaobserwowanymi w czasie pomiarów laboratoryjnych.

Słowa kluczowe:

łuk 90°, odsadzka, rury miedziane, straty miejscowe, modelowanie numeryczne

Keywords:

long elbow 90°, full crossover, copper pipes, minor pressure loss, numerical modeling